analytical chemistry

Article

pubs.acs.org/ac

Sample-to-Answer Isolation and mRNA Profiling of Circulating Tumor Cells

Reza M. Mohamadi,[†] Ivaylo Ivanov,[†] Jessica Stojcic,[‡] Robert K. Nam,[‡] Edward H. Sargent,[§] and Shana O. Kelley*[,†,∥,⊥]

[†]Department of Pharmaceutical Science, Leslie Dan Faculty of Pharmacy, [‡]Division of Urology, Sunnybrook Research Institute, [§]Department of Electrical and Computer Engineering, Faculty of Engineering, [∥]Institute for Biomaterials and Biomedical Engineering, and [⊥]Department of Biochemistry, Faculty of Medicine, University of Toronto, Toronto, Ontario, Canada M5S 3M2

Supporting Information

ABSTRACT: The isolation and rapid molecular characterization of circulating tumor cells (CTCs) from a liquid biopsy could enable the convenient and effective characterization of the state and aggressiveness of cancerous tumors. Existing technologies enumerate CTCs using immunostaining; however, these approaches are slow, labor-intensive, and often fail to enable further genetic characterization of CTCs. Here, we report on an integrated circuit that combines the capture of CTCs with the profiling of their gene expression signatures. Specifically, we use a velocity valley chip to efficiently capture magnetic nanoparticle-bound CTCs, which are then directly analyzed for their gene expression profiles using nanostructured microelectrode biosensors. CTCs are captured with 97% efficiency from 2 mL of whole blood, yielding a 500-fold concentration within 1 h. We show efficient capture of as few as 2 cancer cells/(mL of blood) and demonstrate that the gene expression module accurately profiles the expression of prostate-specific genes in CTCs captured from whole blood. This advance provides the first sample-to-answer solution for gene-based testing of CTCs. The approach was successfully validated using samples collected from prostate cancer patients: both CTCs and prostate-specific antigen (PSA) mRNA sequences were detected in all cancer patient samples and not in the healthy controls.

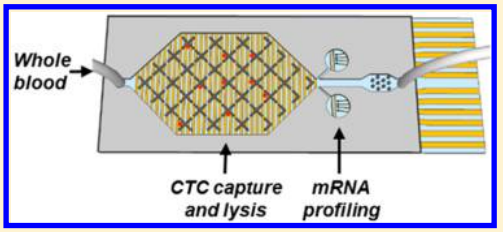

Rapidly growing solid tumors are known to shed circulating tumor cells (CTCs) which can then enter the bloodstream.[1,2] Early, sensitive detection of CTCs may provide a means to facilitate cancer diagnosis and more effectively manage this disease.[3] Furthermore, a better understanding of CTCs' genetic makeup is critical for the development of advanced treatments against metastatic cancer.

The isolation and analysis of CTCs is challenging because CTCs are present at a very low abundance in whole blood. In a blood sample collected from a cancer patient, there can be as few as 1 CTC for every one billion healthy blood cells. Achieving efficient, highly specific capture of CTCs is one of the grand challenges in the field of nanobiotechnology.

In view of the importance of this goal, the development of fluidic devices for CTC capture has become an active and rapidly advancing field.[4−25] Approaches based on affinity capture,[4−9] magnetic isolation,[10−14] and size-based separation[15−17] have been reported, often paired with imaging or conventional off-chip methods for gene expression characterization. Magnetic nanoparticles are a promising class of labels that can be used to target and capture CTCs.[24−26] These nanoparticles can be conjugated to antibodies against cancer markers such as EpCAM to allow for specific binding of CTCs.

Fluorescent immunostaining is routinely used to enumerate CTCs and distinguish them from healthy blood cells. This technique is used in the majority of clinical studies that have proven the importance of CTCs for cancer diagnosis and prognosis as well as showing their predictive value regarding response to treatment.[1−3]

Molecular characterization of CTCs may enable a real-time liquid biopsy that can be periodically acquired in a minimally invasive fashion, thereby allowing a molecular assessment of disease evolution. Present-day approaches for genetic analysis of CTCs are based on fluorescence *in situ* hybridization (FISH), multiplex RT-PCR, microarray, and genomic sequencing or combinations of these methods[27−31] carried out postcapture. The complexity of these techniques is not ideal for routine clinical use, and molecular characterization of cancers is therefore primarily performed on primary tumor tissues rather than CTCs or metastatic tissue.

We present herein an integrated velocity valley (VV) chip that efficiently captures CTCs and allows genetic profiling of captured CTCs from 2 mL of blood within an hour (Figure 1A). Microfabricated X-shaped structures within the fluidic device produce flow VVs, regions of slow flow conducive to labeled cell capture (Figure 1B).[25,26] Antibody-functionalized magnetic nanoparticles selectively label CTCs, allowing for magnetic capture facilitated by external permanent magnets (Figure 1C). Here, we combine this capture approach with *in situ* cell lysis and an electrochemical sensor for mRNA profiling.

Received: March 17, 2015
Accepted: May 26, 2015
Published: May 26, 2015

DOI: 10.1021/acs.analchem.5b01019
Anal. Chem. 2015, 87, 6258−6264

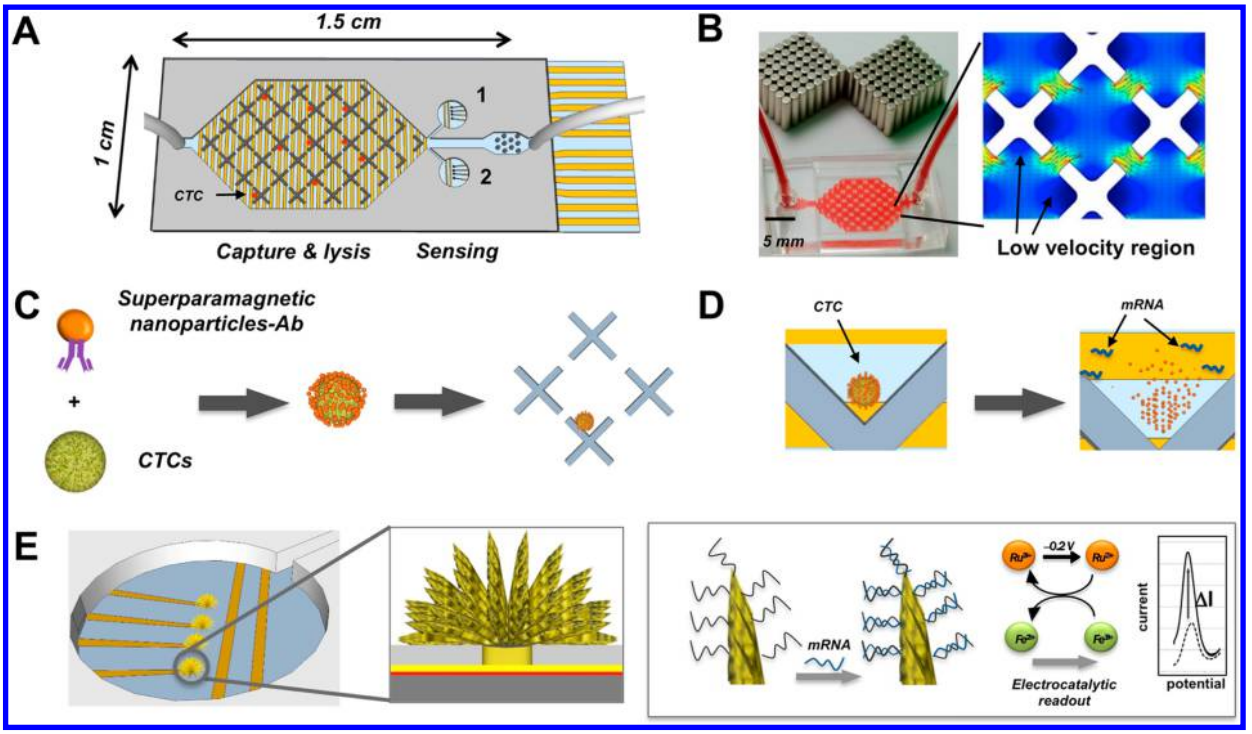

Figure 1. Design of the integrated VV chip. (A) Schematic of the integrated VV chip featuring capture structures, electrochemical lysis electrodes, and nanostructured microelectrode sensors. (B) Photograph of the VV capture device (left) and the flow velocity profile within the capture chamber (right). (C) Target CTCs are labeled with superparamagnetic nanoparticles coated with anti-EpCAM. The labeled cells are then captured in the vicinity of the trapping structures. (D) Electrochemical lysis of the trapped cells achieved using the lysis electrodes. (E) Schematic showing electrochemical sensing of mRNA released from captured CTCs in 1D. Released mRNA hybridizes to PNA probes immobilized on the surface of NMEs. This leads to an increase in current after hybridization as measured by differential pulse voltammetry.

By bringing together nanoparticle-mediated CTC capture, electrochemical cell lysis, and mRNA analysis, we have produced the first sample-to-answer CTC analysis device that is able to profile gene expression in this important class of rare cells.

Previous work in our laboratories on the VV approach for CTC capture focused on a multizone chip that sorted CTCs into subpopulations based on the expression level of EpCAM.[25,26] The cells were then detected using immunostaining. Here, we have tailored the linear velocity and the size of a single-zone chip to capture epithelial CTCs, and incorporated the ability to perform rapid on-chip gene expression analysis. The performance of this integrated device is then showcased using clinical samples, specifically blood samples acquired from prostate cancer patients and healthy controls.

MATERIAL AND METHODS

Capture Chip Preparation. Microchips were fabricated by rapid prototyping using poly(dimethylsiloxane) (PDMS) soft lithography[32] starting with an SU-8 master on a silicon wafer (University Wafer, Boston, MA, USA). A PDMS (Dow Chemical, Midland, MI, USA) replica of the master was formed (channel depth was 50 μm). After peeling the replica, holes were pierced for tubing connections. The replica was permanently sealed with a PDMS-coated glass slide. Bonding was enhanced and made irreversible by oxidizing both the replica and the cover in an oxygen plasma discharge for 1 min prior to bonding. Silicone tubing was then added at the inlet and the outlet.

PDMS chips were conditioned with Pluronic F68 (Sigma-Aldrich, St. Louis, MO, USA) to reduce sample adsorption and washed with PBS pH = 7.4 before use. Two arrays of 56 NdFeB N52 magnets (KJ Magnetics, Pipersville, PA, USA), of 1.5 mm diameter and 8 mm length, were placed on both the bottom and top surfaces of the chip (Figure 1B) for the duration of the cell capture process.

Cell Culture. All cell lines, U937 cells (ATCC catalog no. CRL1593.2), VCaP cells (ATCC catalog no. CRL-2876), and DU145 cells (ATCC catalog no. HTB-81), cell detachment buffer, and media were purchased from ATCC. The cell lines were cultured and prepared according to the protocol suggested by ATCC. The cell lines were characterized for EpCAM protein expression by flow cytometry and also for PSA mRNA expression by RT-PCR. The protocols for cell culture, flow cytometry, and RT-PCR are explained in the Supporting Information.

CTC Capture. Patient blood samples were collected with consent prior to prostate biopsy or radical prostatectomy. The characteristics of these patients are outlined in Supporting Information Table S1. All blood samples were analyzed within a few hours of sample collection. A 40 μL aliquot of anti-EpCAM Nano-Beads (MACS), diameter 50 nm, were added to 2 mL of blood and immediately drawn into the VV chip at a flow rate of 2 mL/h using a syringe pump. The amount of beads used here was sufficient to label a large number of cancer cells ($\sim 10^5$). Next 200 μL of PBS-EDTA at 2 mL/h (6 min) was introduced to remove nontarget cells followed by two wash steps with PBS (200 μL, 2 mL/h for 6 min). After this step, some chips were selected for immunostaining. An extra wash step is often found to be necessary, especially when using patient samples. For mRNA analysis, using either RT-PCR/gel electrophoresis or the NMEs for electrochemical readout, the captured cells were

DOI: 10.1021/acs.analchem.5b01019
Anal. Chem. 2015, 87, 6258−6264

lysed electrochemically as explained in Cell Lysis and Hybridization of mRNA Targets. The lysate was then used for electrochemical sensing of PSA mRNA or RT-PCR.

CellSearch circulating tumor cell analysis on spiked blood samples was performed at the London Health Sciences Centre, London, ON, Canada. Before spiking, cancer cells were counted using an automated cell counter (Countess, Invitrogen, Carlsbad, CA, USA) and recounted with a hemocytometer. The typical error in these counts was 5% to 10% and the final concentration was prepared by serial dilutions in PBS. Since, in the spiked samples, we were targeting a low number of cells, we prepared a single spiked sample in 10 mL of blood for each concentration. From this 10 mL of blood, 2 mL was used in a VV chip and 8 mL was sent to CellSearch for analysis.

Immunostaining. After processing the blood, cells were fixed with 4% paraformaldehyde and subsequently permeabilized with 0.2% Triton X-100 (Sigma-Aldrich) in PBS. Cells were immunostained with antibodies, Alexa-488 Anti-CD45 (Invitrogen) and mouse monoclonal allophycocyanin (APC) antihuman pan-Cytokeratin (GeneTex, Irvine, CA, USA). All of the antibodies were prepared in 100 μL of PBS (final concentration of 5 μg/mL), and staining was performed for 30 min at a flow rate of 0.2 mL/h. Chips were washed between each staining step using 200 μL of 0.1% Triton X-100 in PBS, at 0.6 mL/h for 10 min. Nuclei were stained with 100 μL of DAPI ProLong Gold reagent (Invitrogen; as instructed by the manufacturer, 1 drop/(1 mL of PBS)) at 0.6 mL/h. After completion of staining, all devices were washed with PBS and stored at 4 °C before scanning.

Image Scanning and Analysis. After immunostaining, chips were scanned using a 10× objective and a Zeiss microscope equipped with an automated stage controller and a cooled CCD camera (Hamamatsu, Hamamatsu City, Japan). RGB fluorescent mode was used, with the blue channel used for DAPI (typically 10−30 ms exposure), the green channel for an Alexa 488-labeled CD45 antibody, and the red channel for an APC-labeled cytokeratin antibody (typically 100−300 ms exposure). The exposure time was set individually for each chip and kept constant during the scan. The imaging performed was qualitative (positive/negative) in nature, and therefore the variation of exposure time did not impact the results. Images were acquired with Volocity (PerkinElmer, Waltham, MA, USA) software. Bright field as well as red, green, and blue fluorescence images were recorded. The captured images were then analyzed using a macro prepared in ImageJ,[33] and target and nontarget cells were counted by observation (see Supporting Information for the macro).

Integrated Cell Lysis Electrodes and mRNA Sensing Chip Fabrication. The integrated chip consists of two layers: the top PDMS layer which was fabricated as explained previously and the bottom electrode layer fabricated on a silicon substrate. The devices were fabricated using thin silicon wafers passivated with a thick thermally grown silicon oxide layer. First, using standard photolithographic methods, we patterned positive photoresist to define the structure of electrical contacts and leads. Subsequently, a 500 nm gold layer was deposited using electron-beam-assisted gold evaporation and patterned with a standard lift-off process. Next, a second layer of 500 nm silicon dioxide was deposited to passivate the gold leads using chemical vapor deposition. Finally, 5 μm apertures were etched into the second passivating silicon dioxide layer to expose the gold leads beneath. Interdigitated lysis electrodes were designed and etch in the capture and lysis zone of the chip. The electrodes had 100 μm width and a spacing of 100 μm.

Sensor Fabrication. Chips were washed by sonicating in acetone for 5 min and rinsed with isopropanol (IPA) and water. Nanostructured microelectrodes (NMEs) were electroplated using a standard three-electrode system consisting of a Ag/AgCl reference, Pt auxiliary, and Au working electrode with a 5 μm aperture. The electroplating solution consisted of 20 mM $HAuCl_4$ in 0.5 M HCl. NMEs were plated on the chip using an applied potential of 0 mV relative to reference for 100 s. For the finely nanostructured palladium coating, a second electroplating solution was used (5 mM H_2PdCl_4 in 0.5 M $HClO_4$). The second electroplating step was performed with an applied potential of −250 mV for 10 s. After this step, the PDMS and silicon chip surface were treated with oxygen plasma for 30 s. The two layers were then aligned and irreversibly bonded.

Synthesis and Purification of PNA Probes. A PNA probe for PSA was synthesized in house using a Protein Technologies Prelude peptide synthesizer with sequences specific to PSA mRNA (P12) (NH_2-C-G-D-gtc-att-gga-aat-aac-atg-gag-D-$CONH_2$). The cysteine (C) group ensures specific binding of the PNA to the electrode through a thiol bound.[34] After the synthesis, the probes were purified by HPLC. The probe concentration was determined using a NanoDrop instrument. The molar extinction coefficients were calculated with a program entitled "PNA calculator ver-2.0". The PNA probe for GAPDH (cys-o-gtt-gtc-ata-ctt-ctc) was designed in house and ordered from PNA Bio (PNA Bio, CA).

Functionalization of NMEs with PNA Probes. A solution of 100 nM PNA probe in PBS was deposited on the surface of the NMEs in a dark humidity chamber overnight at room temperature (RT). After probe deposition, free probe was removed by washing for 30 min at room temperature. The background signal (from the probe) was determined by scanning in electrocatalytic solution (10 μM $Ru(NH_3)_6^{3+}$ and 1 mM $Fe(CN)_6^{3-}$) in PBS. Chips were washed with PBS and stored before CTC capture. The functionalized sensors could be kept in the fridge for a week before use.

Cell Lysis and Hybridization of mRNA Targets. After the capture steps, cells were lysed by applying a 20 V potential to the interdigitated electrodes for 5 min. Next, the lysate was transferred to the sensing area and incubated for 30 min. After hybridization, the chips were washed twice with 0.3 × PBS at RT for 5 min. The same catalytic solution was used for the chip scanning before and after hybridization. Electrochemical measurements were made using an Epsilon potentiostat.

Electrochemical Measurements. Electrochemical signals were measured in solutions containing 10 mM $Ru(NH_3)_6^{3+}$, 25 mM sodium phosphate (pH 7), 25 mM sodium chloride, and 1 mM $Fe(CN)_6^{3-}$. Cyclic voltammetry signals before and after hybridization were collected with a scan rate of 100 mV s^{-1}. Limiting reductive current (I) was quantified by subtracting the background at 0 mV from the cathodic current at −350 mV in the cyclic voltammetry signal. Signal changes corresponding to hybridization were calculated as follows: $\Delta I = [(I_{ds} - I_{ss})/I_{ss}] \times 100$ (ss = before hybridization; ds = after hybridization).

RESULTS AND DISCUSSION

Design of an Integrated CTC Capture and Analysis Chip. The integrated VV chip features a capture zone where microfabricated X-shaped structures provide local areas of low flow that facilitate the capture of nanoparticle-tagged cells (Figure 1 and Supporting Information Figure S1). Interspersed

DOI: 10.1021/acs.analchem.5b01019
Anal. Chem. 2015, 87, 6258−6264

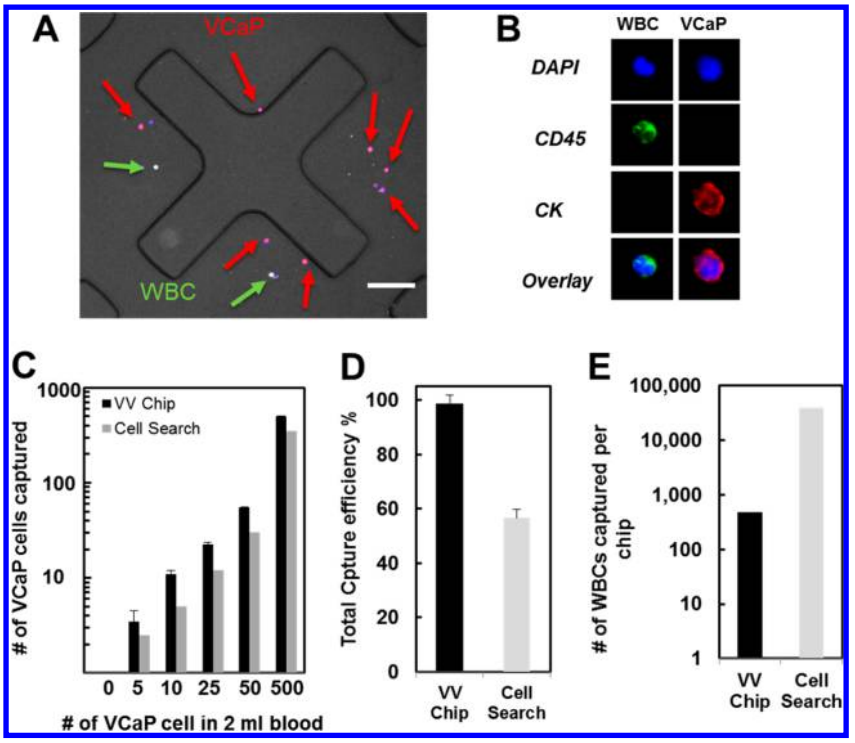

Figure 2. Capture efficiency and electrochemical mRNA sensing of target cells spiked in whole blood in the integrated VV chip. (A) VCaP cells (red) labeled with nanoparticles, captured by the trapping structures. Green arrows indicate white blood cells (WBCs; the scale bar is 200 μm). (B) Fluorescence microscopy of immunostained captured VCaP cells. Cells that are DAPI positive, CD45 negative, and CK positive are counted as cancer cells, while those that are DAPI positive, CD45 positive, and CK negative are WBC. (C) Quantitation of capture efficiencies for VCaP cells spiked into whole blood in a head-to-head comparison of the VV chip with CellSearch. (D) Total capture efficiency. (E) Plot showing average number of WBCs captured per chip in the VV chip was less than 500 while the number of nonspecifically captured WBCs using CellSearch has been reported to be over 40,000.[44]

in this zone are lysis electrodes (Figure 1D). These electrodes transiently generate hydroxide ions that locally increase pH and degrade the cell membranes of captured cells.[35] Once mRNA is released from the captured cells, the lysate flows to a set of nanostructured microelectrodes (NMEs)[36−38] (Figure 1E). The NMEs are gold microelectrodes (~20 μm in diameter) with large surface areas that, through the addition of nanostructured surface features, exhibit high levels of sensitivity (fM − aM) when challenged with nucleic acid analytes.[39] The NMEs are coated with neutral PNA probes specific to complementary mRNA targets. When the mRNA binds to the surface of the NMEs, the sensors become negatively charged. The binding of mRNA and the associated charge change is then amplified and detected using an electrochemical reporter strategy, where two electron acceptors, $Ru(NH_3)^{6+}$ and $Fe(CN)_6^{3-}$, participate in a catalytic reaction that provides a large electrochemical signal corresponding to the level of mRNA bound to the sensor.[40]

Evaluation of Integrated Chip with Blood Samples. To assess the performance of the integrated VV approach in a complex sample, we evaluated samples containing whole, undiluted blood (Figure 2A). We challenged the system with whole blood samples spiked with different numbers of target cancer cells (VCaP). VCaP cells are cultured prostate cancer cells with an epithelial phenotype that express both EpCAM protein on the surface and PSA mRNA within the cell (Supporting Information Figures S2 and S3). Target cells were mixed with 50 nm of magnetic particles coated with anti-EpCAM antibody (Figure 1C). To establish capture efficiency within the chip, the captured cells were fixed and immunostained to distinguish nucleated white blood cells from target cells (Figure 2B). It was observed that, in control blood samples, which did not contain EpCAM-positive cells, most of the traps were empty, whereas when VCaP cells were present in the sample, a significant number of stained cells were visible (Figure 2A). To study this quantitatively, we introduced VCaP cells at levels ranging from 2 to 250 cells/mL. We observed high capture efficiencies at every concentration studied (Figure 2C).

The performance of the velocity valley approach was compared with the gold standard, FDA-cleared, CellSearch assay using spiked blood cells we generated and sent for analysis. At every concentration tested, the velocity valley approach outperformed CellSearch. While the commercially available approach typically offered capture efficiencies of ~60%, the velocity valley devices yielded efficiencies of 97 ± 2% (Figure 2D). When we injected 2 mL of blood, less than 500 (473 ± 22) white blood cells (WBCs) were captured in the VV chip, a nonspecific capture level that is 2 orders of magnitude lower than the typical levels of nonspecific cells captured by CellSearch and significantly lower than other previously reported CTC capture methods (Figure 2E).[4,6] The high rate of capture of nonspecific cells is a limitation of previous systems since these cells interfere with downstream molecular analysis of CTCs.

Immunostaining is widely used for detecting CTCs, but is labor-intensive, slow, and does not provide specific information about the genetic features of cells. We previously reported a chip-based approach to mRNA analysis that is fast and ultrasensitive,[36−42] and we tested its applicability to the analysis

DOI: 10.1021/acs.analchem.5b01019
Anal. Chem. 2015, 87, 6258−6264

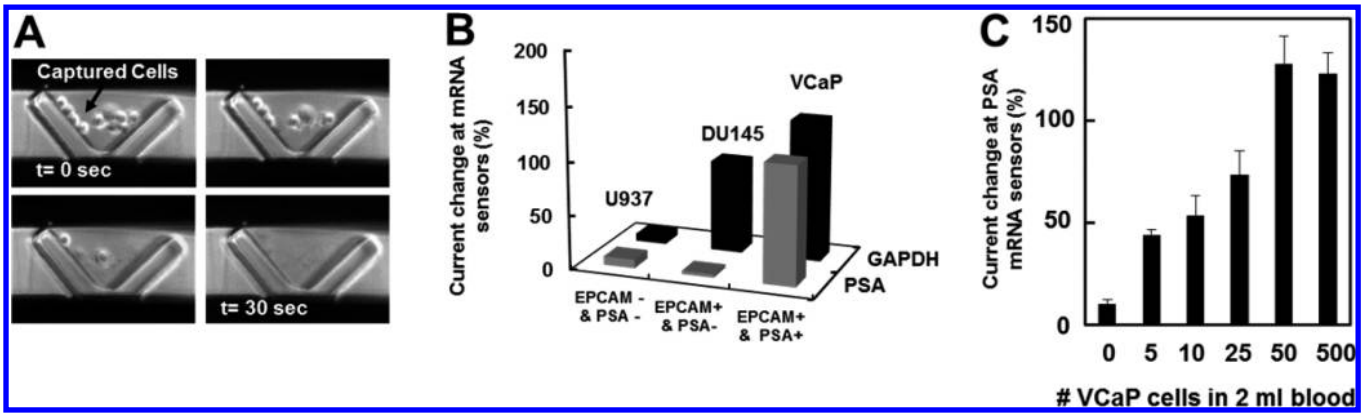

Figure 3. Validation of the integrated VV chip. (A) Electrochemical lysis of captured VCaP cells. (B) Validation of the sensing approach. PSA and GAPDH mRNA hybridize to PNA probes immobilized on the surface of NMEs in two different sensing wells. The specificity of the integrated VV chip was tested with cell lines expressing both EpCAM and PSA (VCaP), only EpCAM but not PSA (DU145), and neither EpCAM nor PSA (U937). (C) Electrochemical signal changes as a function of the number of VCaP cells spiked into 2 mL of blood. The electrochemical reporter system can detect as few as 2 VCaP cells/(mL of blood). Both GAPDH and PSA mRNA were measured in the integrated chip.

of captured CTCs to determine if it could be used to augment the information that could be provided after capture. An integrated device was fabricated that featured a velocity valley chip, electrodes for hydroxide-mediated cell lysis, and mRNA sensors (see Figure 1).

We then immobilized PNA probes on the sensors with sequences complementary to the mRNA that encodes the PSA. PSA was selected to serve as a specific marker for prostate CTCs. We also functionalized a second set of sensors with a probe against GAPDH, a housekeeping gene to be used as a positive control and for signal normalization. We tested the approach with three different cell lines: VCaP, U937, and DU145. U937 is negative for EpCAM, and was used as a double-negative control. DU145 expresses EpCAM but does not express PSA, and was used to mimic the response that would be obtained with a nonprostate derived cell. VCaP is EpCAM positive and expresses PSA, and was included to test the function of both GAPDH and PSA sensors on the chip.

These three different cell types were captured, lysed (Figure 3A), and transferred to a detection chamber that housed the electrochemical sensors for mRNA analysis. The electrochemical signals collected reflected the profiles of each cell type (Figure 3B), validating that this integrated device was effective for the capture, lysis, and genetic analysis of cancer cells.

We challenged the device with low numbers (5−500) of VCaP cells spiked into 2 mL of blood. Using the VV chip, CTCs were captured and lysed, and the crude lysate was analyzed using the on-chip electrochemical sensors (examples of electrochemical readouts are presented in Supporting Information Figure S4). Electrochemical signals were recorded before and after exposure to the sample. When as few as 2 cells were present in 1 mL of blood (or 5 cells in 2 mL of blood), a statistically significant signal change was measured (Figure 3C). The integrity of the released genetic material was also confirmed by conventional PCR (Supporting Information Figure S3).

Testing of Integrated Chip with Prostate Cancer Patient Samples. After testing the VV chip and confirming its capacity for efficient capture of target cancer cells spiked in blood, we tested patient samples collected from prostate cancer patients and healthy controls (16 biopsy-positive prostate cancer patients and 7 healthy controls). The patient samples (2 mL) were incubated with the magnetic nanobeads and introduced directly into the VV chip. Two chips were used for each experiment, one for immunostaining, and one for electrochemical analysis. Immunostained cells were counted as described earlier (Figure 4A,B) and were observed at levels of 15 cells/mL and above for all of the patient samples. In healthy controls, very low cell counts were observed.[6,10,30]

When the mRNA analysis was performed on the blood samples, a statistically significant signal change was observed for all 16 patient samples relative to the control (Figure 4C). With several of the patient samples, multiple runs were performed with the same sample, and excellent run-to-run reproducibility was obtained (Figure 4D). These results indicate that the VV chip, coupled with an electrochemical detection strategy, can be used to detect specific mRNAs in captured CTCs. It is noteworthy, however, that a strong correlation between CTC counts and PSA mRNA electrochemical signals was not present (Supporting Information Figure S5). This may reflect variation in the expression of this gene in different patient's CTCs, as well as the fact that the quantitative capabilities of the assay were not extensively explored in this study. The clinical value of this approach is likely related to the ability to perform rapid, noninvasive screening of patients for CTCs, rather than quantitative analysis of CTCs or disease staging. More extensive studies with higher patient numbers will be required to assess the most appropriate clinical application for the method reported.

■ CONCLUSIONS

The integrated velocity valley chip provides a powerful approach for the sample-to-answer characterization of CTCs at the genetic level directly from patient blood samples within 1 h. Using this device, CTCs are captured with higher efficiency and 2 orders of magnitude higher purity than the FDA-cleared gold standard approach. After capture, the intracellular mRNA is released *in situ* and sent to the adjacent electrochemical sensors for amplification-free rapid genetic analysis. We show that the mRNA from as few as 2 cancer cells can be detected directly from whole blood and validate this approach by profiling a panel of prostate-specific genes from CTCs isolated directly from patient samples. Thus, the integrated VV chip can be applied for rapid monitoring of CTCs in prostate cancer. CTC monitoring has previously been shown to offer improved

DOI: 10.1021/acs.analchem.5b01019
Anal. Chem. 2015, 87, 6258−6264

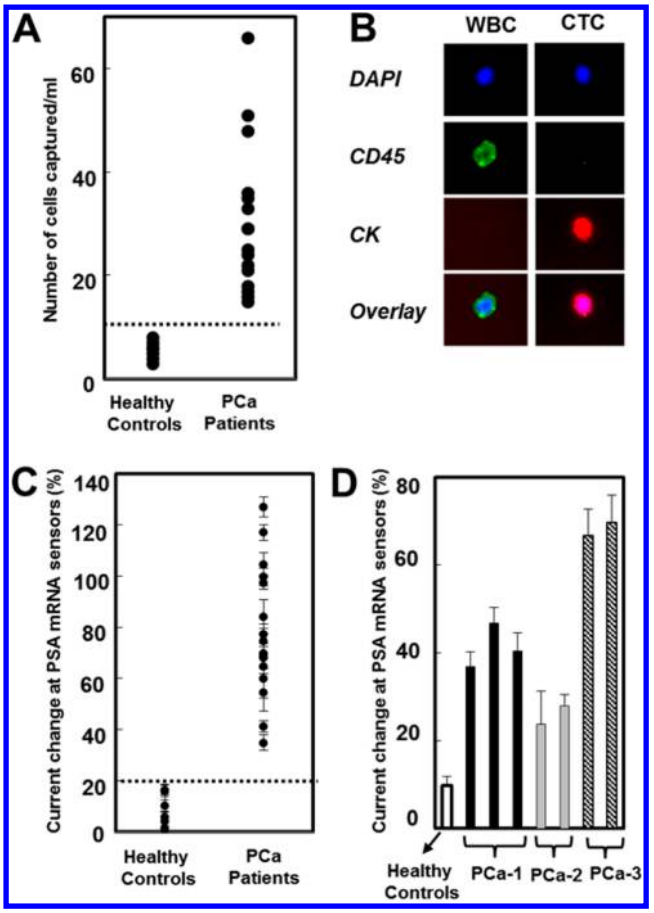

Figure 4. Immunostaining and electrochemical genetic analysis of PSA mRNA from prostate cancer patients in the integrated VV chip. (A) Quantitation of CTCs in patient samples (n = 16) and healthy controls (n = 7) after immunostaining in VV chips (0−7 CK^+ cells were detected in healthy controls). (B) Representative images of a CTC and WBC captured in the VV chip. (C) Electrochemical sensing of PSA mRNA of captured CTCs from the same samples as in A. Each point represents an average of one to three independent capture experiments (2 mL of blood/capture) and three to five electrochemical trials per capture. (D) Chip to chip reproducibility was tested for three patient samples. Error bars represent electrode to electrode reproducibility in the same chip (three to five electrodes).

prediction of metastasis when compared with the routinely used blood PSA test.[43] Although the VV chip provides a rapid means to detect PSA expressing CTCs, the chip in its present form cannot detect mutated CTCs and CTCs which do not express PSA. This limitation could be addressed by increasing the number of on-chip sensors which will allow us to analyze a large panel of biomarkers in the captured CTCs.

■ ASSOCIATED CONTENT

Supporting Information

Experimental details and additional information as noted in the text. The Supporting Information is available free of charge on the ACS Publications website at DOI: 10.1021/acs.analchem.5b01019.

■ AUTHOR INFORMATION

Corresponding Author

*E-mail: shana.kelley@utoronto.ca.

Notes

The authors declare no competing financial interest.

■ ACKNOWLEDGMENTS

We acknowledge the Canadian Institute for Health Research for their generous support of this work through an Emerging Team Grant, the Ontario Research Fund for a Research Excellence Grant, and CMC Microsystems for their support. We extend our appreciation to Justin D. Besant, Adam Mepham, and Andrew T. Sage for their advice throughout the preparation of the manuscript. We thank the ECTI facility at University of Toronto for their cleanroom facilities.

■ REFERENCES

(1) Alix-Panabières, C.; Pantel, K. *Nat. Rev. Cancer* **2014**, *14*, 623−631.
(2) Steeg, P. S. *Nat. Med.* **2006**, *12*, 895−904.
(3) Pantel, K.; Brakenhoff, R. H.; Brandt, B. *Nat. Rev. Cancer* **2008**, *8*, 329−340.
(4) Nagrath, S.; Sequist, L. V.; Maheswaran, S.; Bell, D. W.; Irimia, D.; Ulkus, L.; Smith, M. R.; Kwak, E. L.; Digumarthy, S.; Muzikansky, A.; Ryan, P.; Balis, U. J.; Tompkins, R. G.; Haber, D. A.; Toner, M. *Nature* **2007**, *450*, 1235−1239.
(5) Adams, A.; Okagbare, P. I.; Feng, J.; Hupert, M. L.; Patterson, D.; Go, J. *J. Am. Chem. Soc.* **2008**, *130*, 8633−8641.
(6) Stott, S. L.; Hsu, C.-H.; Tsukrov, D. I.; Yu, M.; Miyamoto, D. T.; Waltman, B. a; Rothenberg, S. M.; Shah, A. M.; Smas, M. E.; Korir, G. K.; Floyd, F. P.; Gilman, A. J.; Lord, J. B.; Winokur, D.; Springer, S.; Irimia, D.; Nagrath, S.; Sequist, L. V.; Lee, R. J.; Isselbacher, K. J.; Maheswaran, S.; Haber, D. A.; Toner, M. *Proc. Natl. Acad. Sci. U. S. A.* **2010**, *107*, 18392−18397.
(7) Yoon, H. J.; Kim, T. H.; Zhang, Z.; Azizi, E.; Pham, T. M.; Paoletti, C.; Lin, J.; Ramnath, N.; Wicha, M. S.; Hayes, D. F.; Simeone, D. M.; Nagrath, S. *Nat. Nanotechnol.* **2013**, *8*, 735−741.
(8) Saliba, A.-E.; Saias, L.; Psychari, E.; Minc, N.; Simon, D.; Bidard, F.-C.; Mathiot, C.; Pierga, J.-Y.; Fraisier, V.; Salamero, J.; Saada, V.; Farace, F.; Vielh, P.; Malaquin, L.; Viovy, J.-L. *Proc. Natl. Acad. Sci. U. S. A.* **2010**, *107*, 14524−14529.
(9) Gleghorn, J. P.; Pratt, E. D.; Denning, D.; Liu, H.; Bander, N. H.; Tagawa, S. T.; Nanus, D. M.; Giannakakou, P. A.; Kirby, B. J. *Lab Chip* **2010**, *10*, 27−29.
(10) Ozkumur, E.; Shah, A. M.; Ciciliano, J. C.; Emmink, B. L.; Miyamoto, D. T.; Brachtel, E.; Yu, M.; Chen, P.; Morgan, B.; Trautwein, J.; Kimura, A.; Sengupta, S.; Stott, S. L.; Karabacak, N. M.; Barber, T. a; Walsh, J. R.; Smith, K.; Spuhler, P. S.; Sullivan, J. P.; Lee, R. J.; Ting, D. T.; Luo, X.; Shaw, A. T.; Bardia, A.; Sequist, L. V.; Louis, D. N.; Maheswaran, S.; Kapur, R.; Haber, D. a; Toner, M. *Sci. Transl. Med.* **2013**, *5*, 179ra47.
(11) Hoshino, K.; Huang, Y.-Y.; Lane, N.; Huebschman, M.; Uhr, J. W.; Frenkel, E. P.; Zhang, X. *Lab Chip* **2011**, *11*, 3449−3457.
(12) Kang, J. H.; Krause, S.; Tobin, H.; Mammoto, A.; Kanapathipillai, M.; Ingber, D. E. *Lab Chip* **2012**, *12*, 2175−2181.
(13) Talasaz, A. H.; Powell, A. a; Huber, D. E.; Berbee, J. G.; Roh, K.-H.; Yu, W.; Xiao, W.; Davis, M. M.; Pease, R. F.; Mindrinos, M. N.; Jeffrey, S. S.; Davis, R. W. *Proc. Natl. Acad. Sci. U. S. A.* **2009**, *106*, 3970−3975.
(14) Casavant, B. P.; Mosher, R.; Warrick, J. W.; Maccoux, L. J.; Berry, S. M. F.; Becker, J. T.; Chen, V.; Lang, J. M.; McNeel, D. G.; Beebe, D. J. *Methods* **2013**, *64*, 137−143.
(15) Zheng, S.; Lin, H. K.; Lu, B.; Williams, A.; Datar, R.; Cote, R. J.; Tai, Y.-C. *Biomed. Microdevices* **2011**, *13*, 203−213.
(16) Hosokawa, M.; Hayata, T.; Fukuda, Y.; Arakaki, A.; Yoshino, T.; Tanaka, T.; Matsunaga, T. *Anal. Chem.* **2010**, *82*, 6629−6635.
(17) Lee, H. J.; Oh, J. H.; Oh, J. M.; Park, J.-M.; Lee, J.-G.; Kim, M. S.; Kim, Y. J.; Kang, H. J.; Jeong, J.; Kim, S. I.; Lee, S. S.; Choi, J.-W.; Huh, N. *Angew. Chem., Int. Ed.* **2013**, *52*, 8337−8340.

DOI: 10.1021/acs.analchem.5b01019
Anal. Chem. 2015, 87, 6258−6264

(18) Wang, S.; Liu, K.; Liu, J.; Yu, Z. T.-F.; Xu, X.; Zhao, L.; Lee, T.; Lee, E. K.; Reiss, J.; Lee, Y.-K.; Chung, L. W. K.; Huang, J.; Rettig, M.; Seligson, D.; Duraiswamy, K. N.; Shen, C. K.-F.; Tseng, H.-R. *Angew. Chem., Int. Ed.* **2011**, *123*, 3140−3144.
(19) Schiro, P. G.; Zhao, M.; Kuo, J. S.; Koehler, K. M.; Sabath, D. E.; Chiu, D. T. *Angew. Chem., Int. Ed.* **2012**, *51*, 4618−4622.
(20) Lien, K.-Y.; Chuang, Y.-H.; Hung, L.-Y.; Hsu, K.-F.; Lai, W.-W.; Ho, C.-L.; Chou, C.-Y.; Lee, G.-B. *Lab Chip* **2010**, *10*, 2875−2886.
(21) Jo, S.-M.; Lee, J.-J.; Heu, W.; Kim, H.-S. *Small* **2014**, *11*, 1975−1982.
(22) Huang, S.-B.; Wu, M.-H.; Lin, Y.-H.; Hsieh, C.-H.; Yang, C.-L.; Lin, H.-C.; Tseng, C.-P.; Lee, G.-B. *Lab Chip* **2013**, *13*, 1371−1383.
(23) Zhao, M.; Schiro, P. G.; Kuo, J. S.; Koehler, K. M.; Sabath, D. E.; Popov, V.; Feng, Q.; Chiu, D. T. *Anal. Chem.* **2013**, *85*, 2465−2471.
(24) Galanzha, E. I.; Shashkov, E. V.; Kelly, T.; Kim, J.-W.; Yang, L.; Zharov, V. P. *Nat. Nanotechnol.* **2009**, *4*, 855−860.
(25) Mohamadi, R. M.; Besant, J. D.; Mepham, A.; Green, B.; Mahmoudian, L.; Gibbs, T.; Ivanov, I.; Malvea, A.; Stojcic, J.; Allan, A. L.; Lowes, L. E.; Sargent, E. H.; Nam, R. K.; Kelley, S. O. *Angew. Chem., Int. Ed.* **2015**, *127*, 141−145.
(26) Besant, J. D.; Mohamadi, R. M.; Aldridge, P. M.; Li, Y.; Sargent, E. H.; Kelley, S. O. *Nanoscale* **2015**, *7*, 6278−6285.
(27) Attard, G.; Swennenhuis, J. F.; Olmos, D.; Reid, A. H. M.; Vickers, E.; A'Hern, R.; Levink, R.; Coumans, F.; Moreira, J.; Riisnaes, R.; Oommen, N. B.; Hawche, G.; Jameson, C.; Thompson, E.; Sipkema, R.; Carden, C. P.; Parker, C.; Dearnaley, D.; Kaye, S. B.; Cooper, C. S.; Molina, A.; Cox, M. E.; Terstappen, L. W. M. M.; de Bono, J. S. *Cancer Res.* **2009**, *69*, 2912−2918.
(28) Yu, M.; Bardia, A.; Wittner, B. S.; Stott, S. L.; Smas, M. E.; Ting, D. T.; Isakoff, S. J.; Ciciliano, J. C.; Wells, M. N.; Shah, A. M.; Concannon, K. F.; Donaldson, M. C.; Sequist, L. V.; Brachtel, E.; Sgroi, D.; Baselga, J.; Ramaswamy, S.; Toner, M.; Haber, D. A.; Maheswaran, S. *Science* **2013**, *339*, 580−584.
(29) Flores, L. M.; Kindelberger, D. W.; Ligon, A. H.; Capelletti, M.; Fiorentino, M.; Loda, M.; Cibas, E. S.; Jänne, P. A.; Krop, I. E. *Br. J. Cancer* **2010**, *102*, 1495−1502.
(30) Stott, S. L.; Lee, R. J.; Nagrath, S.; Yu, M.; Miyamoto, D. T.; Ulkus, L.; Inserra, E. J.; Ulman, M.; Springer, S.; Nakamura, Z.; Moore, A. L.; Tsukrov, D. I.; Kempner, M. E.; Dahl, D. M.; Wu, C.; Iafrate, A. J.; Smith, M. R.; Tompkins, R. G.; Sequist, L. V.; Toner, M.; Haber, D. A.; Maheswaran, S. *Sci. Transl. Med.* **2010**, *2*, No. 25ra23.
(31) Magbanua, M. J. M.; Sosa, E. V.; Scott, J. H.; Simko, J.; Collins, C.; Pinkel, D.; Ryan, C. J.; Park, J. W. *BMC Cancer* **2012**, *12*, No. 78.
(32) Xia, Y.; Whitesides, G. M. *Angew. Chem., Intl. Ed.* **1998**, *37*, 550−575.
(33) Schneider, C. A.; Rasband, W. S.; Eliceiri, K. W. *Nat. Methods* **2012**, *9*, 671−675.
(34) Love, J. C.; Estroff, L. A.; Kriebel, J. K.; Nuzzo, R. G.; Whitesides, G. M. *Chem. Rev.* **2005**, *105*, 1103−1169.
(35) Besant, J. D.; Das, J.; Sargent, E. H.; Kelley, S. O. *ACS Nano* **2013**, *7*, 8183−8189.
(36) Soleymani, L.; Fang, Z.; Lam, B.; Bin, X.; Vasilyeva, E.; Ross, A. J.; Sargent, E. H.; Kelley, S. O. *ACS Nano* **2011**, *5*, 3360−3366.
(37) Kelley, S. O.; Mirkin, C. A.; Walt, D. R.; Ismagilov, R. F.; Toner, M.; Sargent, E. H. *Nat. Nanotechnol.* **2014**, *9*, 969−980.
(38) Sage, A. T.; Besant, J. D.; Lam, B.; Sargent, E. H. *Acc. Chem. Res.* **2014**, *47*, 2417−2425.
(39) Soleymani, L.; Fang, Z.; Sargent, E. H.; Kelley, S. O. *Nat. Nanotechnol.* **2009**, *4*, 844−848.
(40) Lapierre, M. A.; O'Keefe, M. M.; Taft, B. J.; Kelley, S. O. *Anal. Chem.* **2003**, *75*, 6327−6333.
(41) Vasilyeva, E.; Lam, B.; Fang, Z.; Minden, M. D.; Sargent, E. H.; Kelley, S. O. *Angew. Chem., Int. Ed.* **2011**, *50*, 4137−4141.
(42) Ivanov, I.; Stojcic, J.; Stanimirovic, A.; Sargent, E. H.; Nam, R. K.; Kelley, S. O. *Anal. Chem.* **2013**, *85*, 398−403.
(43) Danila, D. C.; Fleisher, M.; Scher, H. I. *Clin. Cancer Res.* **2011**, *17*, 3903−3912.
(44) Miller, M. C.; Doyle, G. V.; Terstappen, L. W. M. M. *J. Oncol.* **2010**, *2010*, No. 617421.

DOI: 10.1021/acs.analchem.5b01019
Anal. Chem. 2015, 87, 6258−6264